
Transformer-based Planning for Symbolic Regression

Parshin Shojaee*¹, Kazem Meidani*²
Amir Barati Farimani^{2,3}, Chandan K. Reddy¹

¹ Department of Computer Science, Virginia Tech

² Department of Mechanical Engineering, Carnegie Mellon University

³ Machine Learning Department, Carnegie Mellon University

Abstract

Symbolic regression (SR) is a challenging task in machine learning that involves finding a mathematical expression for a function based on its values. Recent advancements in SR have demonstrated the efficacy of pretrained transformer-based models for generating equations as sequences, which benefit from large-scale pre-training on synthetic datasets and offer considerable advantages over GP-based methods in terms of inference time. However, these models focus on supervised pretraining goals borrowed from text generation and ignore equation-specific objectives like accuracy and complexity. To address this, we propose TPSR, a **Transformer-based Planning strategy for Symbolic Regression** that incorporates Monte Carlo Tree Search into the transformer decoding process. TPSR, as opposed to conventional decoding strategies, allows for the integration of non-differentiable feedback, such as fitting accuracy and complexity, as external sources of knowledge into the equation generation process. Extensive experiments on various datasets show that our approach outperforms state-of-the-art methods, enhancing the model's fitting-complexity trade-off, extrapolation abilities, and robustness to noise. We also demonstrate that the utilization of various caching mechanisms can further enhance the efficiency of TPSR.

1 Introduction

Symbolic regression (SR) is a powerful method to discover mathematical expressions for governing equations of complex systems and to describe data patterns in an interpretable symbolic form. It has been widely used in various applications of science and engineering to model physical phenomena such as those in molecular dynamics, fluid dynamics, and cosmology [1–6]. Symbolic representations provide insights into complex systems and help us better understand, predict, and control the systems by designing accurate, generalizable, and efficient models of them [7–9]. SR models map the pair of independent and target variables to the mathematical equations that describe the functional relationship between these variables. The input data can be obtained from simulations, experimental measurements, or real-world observations. Symbolic regression is a challenging task due to several reasons including the combinatorial nature of the optimization search space, input data quality, and difficulty in maintaining the balance between the model fitting, complexity, and generalization performance [10, 11].

There are various categories of methods for the SR problem. Traditional approaches, such as Genetic Programming (GP), use a heuristic population-based search strategy where each individual represents a potential solution to the problem [12, 13]. Though GP algorithms are capable of finding solutions for nonlinear and complex problems, they are typically slow to converge due to the large functional search space. Also, as they start the search from scratch for each given equation, they are usually computationally expensive, prone to overfitting, and sensitive to the choice of parameters [14]. Recent

*Equal contribution. Contact email: parshinshojaee@vt.edu

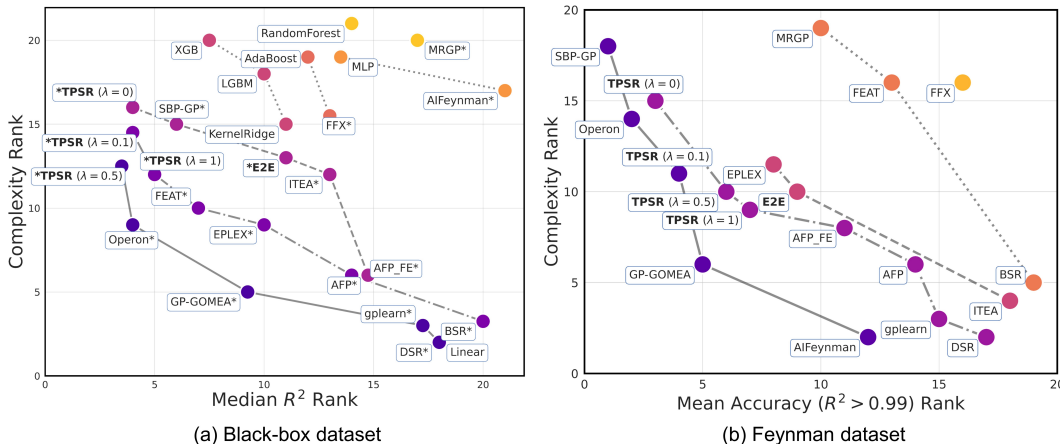


Figure 1: Pareto plot comparing the rankings of all methods in terms of the R^2 performance and identified equation complexity for (a) **SRBench Black-box dataset** and (b) **Feynman dataset**. Our results with Transformer-based Planning (TPSR) applied on top of E2E transformer SR model improves its average accuracy on both datasets while maintaining a similar range of equation complexity. *TPSR can successfully reach the first Pareto-front which is better than E2E baseline on both datasets.* Connecting lines and color denote Pareto dominance rankings and "*" indicates SR methods.

works in SR have shown promising results by using pretrained language models based on transformers [15] for generating equations as sequences. These models leverage the large-scale pretraining and can generate equations with a single forward pass, leading to faster inference times compared to GP-based methods. The transformer-based SR models can generate equation skeletons [16, 17] or complete equations with constants [18, 19], and refine them for a better data fit [20]. However, one of the limitations of these models is that they focus on the supervised pretraining goals borrowed from text generation, i.e., they are trained solely with the token-level cross-entropy (CE) loss, which can result in equations that may exhibit high token-level similarities but are suboptimal with respect to equation-specific objectives such as fitting accuracy and complexity. To mitigate this issue, beam search [21, 22] or sampling [23] approaches are employed as decoding strategies to propose multiple candidate equations for a given dataset, and then select the optimal candidate equation based on the fitting accuracy after optimizing for constants. However, both beam search and sampling decoding strategies primarily rely on the pretrained transformer’s logits and next token probability distributions, and therefore do not receive any performance feedback on their generated equation candidates.

To consider the equation-specific objectives in the transformer generation process and still benefit from the pretrained model logits, we propose TPSR, a **T**ransformer-based **P**lanning strategy for **S**ymbolic **R**egression. TPSR leverages a lookahead planning algorithm, using Monte Carlo Tree Search (MCTS) as a decoding strategy on top of pretrained transformer-based SR models to guide equation sequence generation. TPSR significantly improves the performance of generated equations by considering feedback during the generation process and still remains faster than GP-based models which do not leverage the pretraining priors and learn each equation sample from scratch. Notably, our approach is model-agnostic and can be applied to any pretrained SR model, enabling optimization of generated equation sequences for non-differentiable objectives that may encompass combinations of fitting accuracy, complexity, and equation forms. Additionally, we incorporate different caching mechanisms to reduce the overall inference time. Our experimental results demonstrate that applying TPSR on top of the pretrained E2E SR model [18] significantly enhances its performance across various benchmarks, including the *Feynman* dataset [24] and SRBench *Black-box* dataset [25]. As depicted in Fig. 1, TPSR achieves a strong balance between fitting accuracy and model complexity compared to other leading baselines. It also effectively drives the E2E model towards the optimal trade-off, represented by the first Pareto front, on both datasets. The major contributions of this work are summarized below:

- Propose TPSR, a new method that combines pretrained transformer SR models with Monte Carlo Tree Search (MCTS) lookahead planning to optimize the generation of equation sequences while considering performance feedback.

- Develop a new reward function that balances equation fitting accuracy and complexity to optimize the generated equations for an effective trade-off.
- Demonstrate that TPSR consistently outperforms state-of-the-art baselines across various SR benchmark datasets, generating equations with higher fitting accuracy while maintaining lower complexity to avoid non-parsimonious solutions.
- We also showcase the extrapolation and noise robustness of TPSR compared to the baseline and conduct an ablation study to investigate the impact of the various model components.

The rest of this paper is organized as follows: Section 2 summarizes existing SR methods including GP-based single-instance search and transformer-based pretrained models as well as the existing planning-based sequence generation methods. The details of our proposed TPSR method are presented in Section 3. In Section 4, we evaluate our method on standard SR datasets and perform an ablation study and qualitative case study. Finally, the paper concludes in Section 5.

2 Related Works

Single-Instance Symbolic Regression. For the problem of single-instance SR, Genetic Programming (GP) algorithms are commonly used to find the best-fit equation for a given function’s observations [12]. Recently, the use of neural networks was explored as an alternative search algorithm. One approach is to use deep reinforcement learning (RL) [14, 26, 27] to improve the equation search process through policy gradient optimization of a policy network that outputs a sequence of tokens. Another approach is a combination of GP and RL [28], where the policy network is used to seed the GP algorithm’s starting population. It is worth mentioning that Monte Carlo Tree Search (MCTS) has also been recently employed as a stand-alone framework for SR from scratch as it can provide a flexible way to represent the search space with customized production rules to guide the search tree expansion [29]. However, all these methods lack the advantages of large-scale pretraining and are slow during inference, since they have to retrain the search from scratch for each new dataset. The SRBench, introduced by [25], is a benchmarking framework for SR that includes 14 methods, including GP- and RL-based approaches, evaluated on real-world and synthetic regression datasets.

Pretrained Transformers for Symbolic Regression. In recent years, pretrained language models have shown remarkable performance in natural language and programming language tasks [30–32]. This success has inspired researchers to propose experience-based pretrained transformer models for SR. For example, Biggio *et al.* [16] introduced a Neural Symbolic Regression (NSR) model that scales with the amount of synthetic training data and generates equation skeletons where all the numerical constants are represented by a single token “C”. Similarly, Valipour *et al.* [17] proposed SymbolicGPT, a character-level model for equation skeleton generation. Kamienny *et al.* [18] proposed an end-to-end framework that predicts the complete equation form along with its constants and Vastl *et al.* [19] introduced a model that encodes constants by their scales, providing a middle ground for constant tokenization. These approaches leverage the power of large-scale pretraining with synthetic data to generate accurate and compact equations for SR problems. However, existing transformer-based models are only trained on token-level cross-entropy loss, resulting in suboptimal equations for other equation-specific objectives such as fitting accuracy and complexity. Decoding strategies such as beam search or sampling are used to propose multiple candidate equations, but they do not receive performance feedback on generated equations until the entire sequence is generated. Our model, TPSR, utilizes MCTS lookahead planning to guide the generation of equations towards better performance by employing fitting and complexity feedback during the generation process.

Planning in Sequence Generation. Recently, natural language processing (NLP) tasks have utilized planning algorithms such as Monte Carlo Tree Search (MCTS) to determine the best text output for a given objective, defined as a reward function. For instance, Scialom *et al.* [33] used MCTS with a pretrained discriminator as the reward to optimize language GANs. Leblond *et al.* [34] and Chaffin *et al.* [35] recently employed MCTS as a decoding strategy for controllable text generation by taking a given constraint, such as being non-toxic or conveying certain emotions, as the reward and optimizing text to meet that constraint. Recent advances in programming language models developed in the field of code generation have also shown promising techniques that could be adapted for symbolic regression, as they share several vital similarities with each other. Both involve generating sequences of symbols for a given input and typically require optimizing the generated

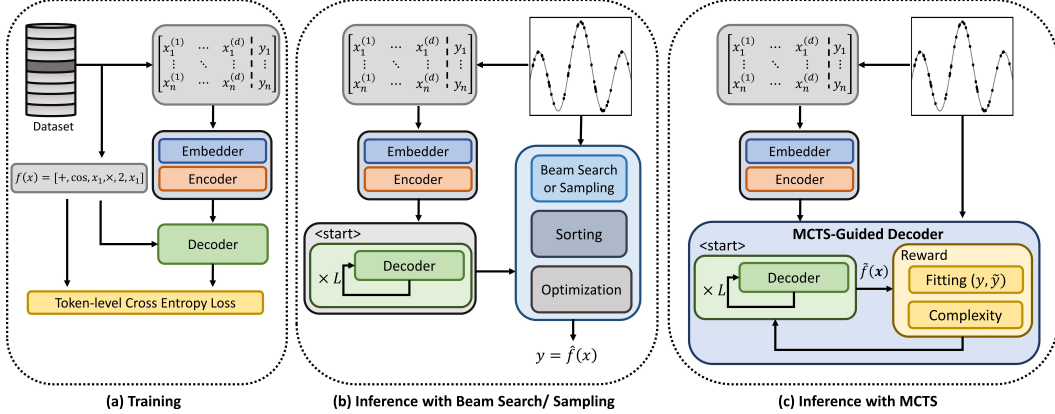


Figure 2: An overview of our proposed method with MCTS-guided decoding at inference compared to the concurrent works with beam search/sampling decoding strategy.

sequences for specific criteria. For code generation, this may involve optimizing objectives like code compilability, readability, or passing test cases [36, 37]. Similarly, in symbolic regression, the focus may be on equation-specific sequence-level objectives such as fitting accuracy or minimizing complexity. MCTS-guided decoding has also recently been used for code generation to optimize pretrained programming language models to generate codes with higher test case pass rates [38]. Motivated by these success stories, in this work, we develop a similar approach in the context of symbolic regression, with the goal of generating equations that exhibit better fitting accuracy or more desirable forms. Our work is the first to combine MCTS with transformer-based SR models to generate enhanced equations for a given dataset by utilizing performance feedback in generation with lookahead planning. We successfully constructed the coupling between these two components and overcame the distinct challenges involved in optimizing the framework. We also implemented different caching mechanisms to further improve our framework’s computational efficiency.

3 The Proposed TPSR Method

3.1 Preliminaries

In Symbolic Regression (SR), the main goal is to find a symbolic expression for the unknown function $f(\cdot)$ mapping the d -dimensional input $\mathbf{x} \in \mathbb{R}^d$ to the target variable $y = f(\mathbf{x}) \in \mathbb{R}$. Given a dataset of n observations $\mathcal{D} = (\mathbf{x}_i, y_i)_{i=1}^n$, SR methods try to generate an equation $\hat{f}(\cdot)$ such that $y_i \approx \hat{f}(\mathbf{x}_i)$ for all $i \in \mathbb{N}_n$. Also, the proposed equation is desired to generalize well and to effectively balance the fitting accuracy and complexity.

The deep learning-based and transformer-based SR models are trained on a large-scale dataset of equation instances $\{(\mathcal{D}_1, f_1(\cdot)) \dots (\mathcal{D}_M, f_M(\cdot))\}$, where M is the dataset size. During inference, given the observations \mathcal{D}_{test} , the learned model directly generates the equation $\hat{f}(\cdot)$ as a sequence of tokens in an autoregressive manner, with each subsequent token generated based on the preceding ones. An effective way to represent the expression trees of equations in a sequence is to use prefix notation as in [39]. Transformer-based models first embed and encode the input observations, and then pass the encoded representation along with the masked tokens to generate the equation sequence. To train the model, token-level cross-entropy loss is employed to learn the distribution of next token prediction conditioned on the encoded dataset and the current state of sequence (Figure 2(a)).

Achieving a good fitting performance from the model’s predicted sequence demands generating accurate constants in the equation which is challenging. To address this, the generated skeleton or equation can undergo a round of optimization to estimate their constants using nonlinear methods, such as Broyden–Fletcher–Goldfarb–Shanno algorithm (BFGS) [20]. While using constant optimization improves the fitting quality of the generated equation, we should note that searching over the constants of output sequences in a greedy manner can reduce the model’s flexibility by not considering other possible candidates that might perform better than the greedy solution. Previous works [16, 18] employ beam search and sampling strategies for transformer decoding in combination with constant optimization to propose several candidate equations. Subsequently, they use fitting

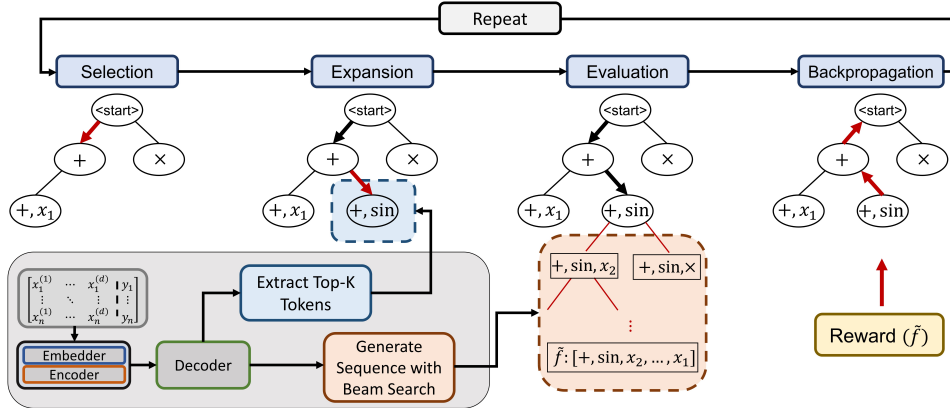


Figure 3: Overview of TPSR’s key steps: Selection, Expansion, Evaluation, and Backpropagation. MCTS-guided decoding interacts with the pretrained transformer SR model in the expansion and evaluation steps employing the transformer $top-k$ sampling and beam search, respectively. Then, the value of a node is obtained as the highest reward of all simulations and the reward is used to guide the backpropagation.

metrics such as R^2 (i.e., R-squared) to order these candidates and output the final equation with the best performance (Figure 2(b)). Transformer models utilizing beam search or sampling decoding strategies can generate multiple high-likelihood equation sequences, but they rely on logits obtained from model parameters pretrained with token-matching loss relative to the reference equation. As a result, such models lack the capability to receive feedback and optimize for sequence-level objectives such as fitting or complexity of equations.

3.2 MCTS-Guided Equation Generation

To generate equations that are both better-fitting and less-complex, it is crucial to incorporate feedback into the equation generation process. To achieve this, we utilize Monte Carlo Tree Search (MCTS) during inference time to guide the decoder towards optimal solutions for fitting and complexity objectives (as shown in Figure 2(c)). This MCTS-guided transformer decoding allows exploring different possibilities and identifying the most promising paths, based on the designed objective.

To this end, we first formulate the SR equation generation task as a Markov Decision Process (MDP) where the state s is the current incomplete or complete sequence at iteration t of generation. If s has not reached the terminal state (i.e., the $\langle end\ of\ sentence \rangle$ token), we proceed with the generation by selecting the next token from vocabulary as the action a . Therefore, the updated state s' will be obtained from the concatenation of s and a . Once the terminal action is reached, i.e., the entire equation sequence is generated, the reward r will be computed and used to update the decoding model. As shown in Fig. 3, MCTS represents states as nodes and actions as edges in a tree structure. Starting from the root node (i.e., initial state), MCTS navigates through the state-space to reach terminal states with the maximum reward. This algorithm keeps track of the number of visits to each node and the value function of each edge. During the node selection process, MCTS considers two key criteria: firstly, it looks for nodes with higher quality equations (i.e., higher Q-values), and secondly, it prioritizes under-explored nodes (i.e., those with a smaller number of visits). By incorporating these two selection criteria, MCTS can balance between exploration and exploitation.

During the generation process of the transformer, we utilize the MCTS algorithm iteratively to conduct lookahead planning and determine the next token. However, the large search-space requires more than the sole application of MCTS to generate high-quality equations. We need to effectively share information between the pretrained transformer model and MCTS for better generations. To achieve this, we incorporate the probabilities of the next-token that are acquired through the pretrained transformer SR models into the MCTS planning process. This incorporation helps to enhance the search process, leading to more efficient and effective results. The key steps of the MCTS algorithm that we utilize for transformer decoding in SR models are depicted in Fig. 3 and are as follows:

Selection. In the selection stage, a common node selection criterion, Upper Confidence Bound for Trees (UCT) [40], is employed to select the actions (i.e., next tokens) for fully extended nodes in the search tree. A node is considered fully extended if it has at least k children to prevent excessive time consumption. UCT aims to balance the exploration of less-visited states and the exploitation of known-to-be-good states, striking a trade-off between the two.

$$\text{UCT}(s, a) = Q(s, a) + \beta \sqrt{\frac{\ln(N(s))}{N(s')}},$$

where $Q(s, a)$ is the maximum return/reward of playing action a in state s in all the performed simulations, which encourages exploitation of the current best child node. Furthermore, the algorithm promotes the exploration of less-visited child nodes through the second term, $\sqrt{\frac{\ln(N(s))}{N(s')}}$, where $N(s)$ is the number of times state s is visited, and s' is the next state obtained by taking action a in the current state s . The hyperparameter β controls the balance between exploration and exploitation, where greater β values promote more exploration. The selected next token action is to maximize the UCT. Hence,

$$\text{Select}(s) = \arg \max_a \text{UCT}(s, a).$$

Expansion. In the expansion stage, after selecting a node that is not fully expanded, a new child (next token) for the current state is explored. Random expansion of the node from the vocabulary, however, might result in an invalid equation (that does not comply with the prefix notation) and makes the process very time-consuming. Therefore, given partial equations, only *top-k* most likely choices of the next token are considered as the possible children of the node for expansion. In other words, we are restricting the actions to be only from the *top-k* high-likelihood options which are retrieved from the pretrained transformer SR model’s logits. These options are then ordered to determine the sequence in which the children will be expanded.

Evaluation. To evaluate the newly expanded nodes, we perform simulations to complete the equation sequence. This is necessary because the new state may still be a partial equation and performance feedback can only be obtained at the end of the sequence when the equation generation is completed. In MCTS, it is common to employ random actions during the simulation stage. Nevertheless, random action selection for equation generation, much like during expansion, suffers from certain drawbacks in terms of time and the possibility of generating invalid equations. Consequently, the pretrained transformer SR model is invoked again, this time utilizing beam search with a beam size of b , to generate complete equation candidates based on the current state. The beam size b determines the number of complete equations to be generated from the current partial equation. Following the simulations, the highest reward among all the candidates is assigned to the new node value.

Backpropagation. After generating a complete equation $\tilde{f}(\cdot)$, the corresponding reward $r(\tilde{f}(\cdot))$ can be computed. The highest reward among all simulations is then assigned to the new node, which recursively backpropagates its estimated value to its parents until it reaches the root of the tree. This update process involves updating the Q values of all state-action pairs, denoted as s' and a' , along the trajectory in the tree to reach the new state. Specifically, for each state-action pair, the Q value is updated by taking the maximum of the current Q value and the estimated value v : $Q(s', a') \leftarrow \max(Q(s', a'), v)$.

3.3 Reward Definition

To evaluate the complete equation candidate $\tilde{f}(\cdot)$, we define numerical reward $r \in \mathbb{R}$ which promotes fitting accuracy and regularizes the equation’s complexity. Also, to effectively evaluate the fitting performance, we compute the reward after optimizing the constants of the complete sequence. We first calculate the normalized mean squared error (NMSE) between the ground-truth target variable y and the predicted target variable $\tilde{y} = \tilde{f}(\mathbf{x})$:

$$\text{NMSE}(y, \tilde{f}(\mathbf{x})) = \frac{\frac{1}{n} \|y - \tilde{f}(\mathbf{x})\|_2^2}{\frac{1}{n} \|y\|_2^2 + \epsilon},$$

where ϵ is a small real value to avoid numerical instability. In our study, we consider the general form of the reward as

$$r(\tilde{f}(\cdot)|\mathbf{x}, y) = \frac{1}{1 + \text{NMSE}(y, \tilde{f}(\mathbf{x}))} + \lambda \exp\left(-\frac{l(\tilde{f}(\cdot))}{L}\right), \quad (1)$$

where l denotes the complexity of the equation which is defined (in earlier works [16, 18, 25]) as the sequence length of the equation represented in prefix notation; L indicates the maximum possible length of the sequence in the model; and λ is a hyperparameter that controls the balance between fitting and complexity reward. Higher values of λ promote equations that are less complex. Therefore, This reward function is designed to encourage best-fitting and penalize non-parsimonious solutions.

3.4 Efficient Implementation with Caching

During the evaluation step of MCTS, the transformer model is utilized to generate complete sequences from a given state. This process involves constructing implicit tree structures to perform beam search, which entails computing the $top-k$ next tokens for the visited states during generation until the entire sequence is generated. These computations will be required again in future MCTS iterations to extract the $top-k$ next tokens during the expansion step of each state, and generate the complete equation from a given state during the evaluation step. Therefore, two caching mechanisms, namely $top-k$ caching and sequence caching, are employed to prevent redundant computations and enhance the efficiency of our framework.

The $top-k$ caching mechanism involves the storage of computed $top-k$ values for the given states. For instance, when we evaluate the state $s = [+ , \sin]$ in iteration t of MCTS, the $top-k$ tokens are computed for s and its subsequent visited states (e.g., $[+ , \sin, x_2]$). The pairs of states and their corresponding $top-k$ values can be stored in a $top-k$ cache. Therefore, if a state s is visited again in a future iteration (e.g., visiting $s = [+ , \sin, x_2]$ in iteration $t + 1$ of MCTS), the cached $top-k$ values are used instead of retrieving the $top-k$ tokens from the model.

The caching of complete equations generated in a greedy manner is another mechanism employed to reduce redundant computations. When the beam size in MCTS is one, the sequence is generated greedily for the given state in the evaluation step. It means that if any partial sequence of this equation is given, the same equation will be generated by the decoder. Therefore, the generated equation in iteration t can be directly used in future iterations if the state matches the stored equation partially. For example, consider the equation $\tilde{f} : [+ , \sin, x_2, \cdot, x_1]$ is generated for $s = [+ , \sin]$ with $b = 1$ in iteration t . Now, if in a later iteration (e.g., iteration $t + 1$), the state to evaluate is $s = [+ , \sin, x_2]$, we can bypass the iterative sequence generation process by directly using the sequence cache to predict the complete equation. It is worth noting that both of these caching strategies serve the same purpose of enhancing the framework’s efficiency without compromising its performance.

4 Experiments

In this section, we present our experimental results that evaluate the effectiveness and efficiency of TPSR. While the proposed decoding strategy is generally model-agnostic, i.e., it can be used with any other pretrained deep SR model, here we showcase the results of using TPSR for the end-to-end (E2E) SR transformer model [18]. We evaluate our framework by answering the following research questions (RQs):

- **RQ1:** Does TPSR perform better than other decoding strategies (beam search/sampling) and competing baselines over standard SR benchmark datasets?
- **RQ2:** Does TPSR provide better extrapolation and robustness to noise?
- **RQ3:** Are TPSR’s caching mechanisms effective in saving the computation time?
- **RQ4:** What’s the role of individual MCTS components in TPSR’s overall performance gain?

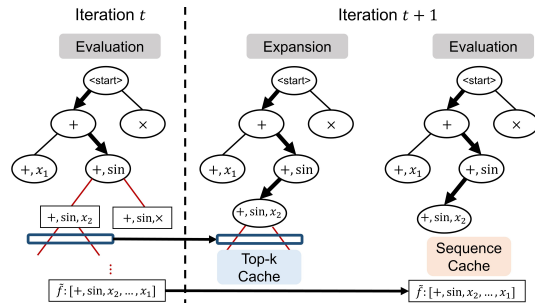


Figure 4: An illustration of caching mechanisms in TPSR. The red edges in the tree indicate beam search simulations performed to find complete equation candidates.

4.1 Datasets

We evaluate TPSR and several baseline methods on the following four standard benchmark datasets: *Feynman*, *Black-box*, and *Strogatz* from SRBench [25], and *In-domain Synthetic Data* generated based on [18]. More details on each of these datasets are given below.

Feynman²: This dataset contains 119 equations sourced from *Feynman Lectures on Physics database* series [41]. The regression input points (x, y) from these equations are provided in Penn Machine Learning Benchmark (PMLB) dataset [25, 42] and have been studied in SRBench [25] for the symbolic regression task. The input dimension is limited to $d \leq 10$ and the true underlying function of points is known. We split the dataset into B bags of 200 input points (when N is larger than 200) since the transformer SR model is pretrained on $N \leq 200$ input points as per [18].

Strogatz³: This dataset comprises 14 symbolic regression problems sourced from the *ODE-Strogatz database* [43] for nonlinear dynamical systems. The input points for these problems are included in PMLB [42] and have been examined in SRBench [25] for symbolic regression. The input dimension for these problems is restricted to $d = 2$ and the true underlying functions are provided.

Black-box⁴: The black-box regression datasets from PMLB [42] are used for the symbolic regression task and studied in SRBench [25] among various baselines. The aim of SR study on these black-box datasets is to find an interpretable model expression that fits the data effectively. We limit the datasets to those with continuous features and input dimension $d \leq 10$, as the transformer SR model [18] is pretrained with $d_{max} = 10$. In total, there are 57 black-box datasets that consist of real-world and synthetic datasets with varying levels of noise.

In-domain Synthetic Data: Following [18], we construct a fixed validation set consisting of 400 equation examples in which the validation functions were uniformly distributed across three different difficulty factors: input dimension (d), number of unary operators (u), and binary operators (b). Specifically, we set $d \sim \mathcal{U}(1, d_{max})$, $b \in \mathcal{U}(d - 1, d + b_{max})$, and $u \sim \mathcal{U}(0, u_{max})$, where $d_{max} = 10$, $u_{max} = 5$, and $b_{max} = 5 + d$. The equation sequence is generated for each function by providing $N = [50, 100, 150, 200]$ input points (x, y) , and the prediction accuracy is assessed on $N_{test} = 200$ points that are randomly extracted from a multimodal distribution, as described in [18]. This data is referred to as “in-domain” because the validation data is generated using the same approach as the data on which the model [18] is pretrained.

4.2 Evaluation Metrics

We evaluate our model using the following three metrics: R^2 score [25], accuracy to tolerance ω [16, 44], and equation complexity [18, 25].

$$R^2 = 1 - \frac{\sum_i^{N_{test}} (y_i - \tilde{y}_i)^2}{\sum_i^{N_{test}} (y_i - \bar{y})^2}, \quad Acc_\omega = \mathbb{1}\left(\max_{1 \leq i \leq N_{test}} \left| \frac{\tilde{y}_i - y_i}{y_i} \right| \leq \omega\right), \quad Complexity = \left| \mathcal{T}(\tilde{f}(\cdot)) \right|,$$

where R^2 measures the performance of fitting, while Acc_ω evaluates precision for the generated equations based on a desired tolerance threshold ω . Equation complexity is also determined by the number of nodes in the expression tree \mathcal{T} of the generated equation $\tilde{f}(\cdot)$, i.e., $\left| \mathcal{T}(\tilde{f}(\cdot)) \right|$. Following [18, 25], to address potential issues with R^2 and Acc_ω , we set $R^2 = 0$ for rare pathological examples and discard the worst 5% predictions for Acc_ω to reduce sensitivity to outliers.

4.2.1 (RQ1) Effectiveness of TPSR

Table 1 presents the performance comparison results of TPSR with the baseline decoding strategies on the SRBench benchmark and the in-domain synthetic dataset. For the E2E baseline, we use the settings reported in [18], including beam/sample size of $C = 10$ candidates, and the refinement of all the candidates $K = 10$. For our model, we use the width of tree search as $k_{max} = 3$, number of rollouts $r = 3$, and simulation beam size $b = 1$ as the default setting. For PMLB datasets that contain

²<https://space.mit.edu/home/tegmark/aifeynman.html>

³<https://github.com/lacava/ode-strogatz>

⁴<https://github.com/EpistasisLab/pmlb/tree/master/datasets>

Data Group	Model	Feynman		Strogatz		Black-box	
		$\uparrow R^2 > 0.99$	$\downarrow Complexity$	$\uparrow R^2 > 0.99$	$\downarrow Complexity$	$\uparrow R^2$	$\downarrow Complexity$
SRBench	E2E+Beam	0.815	54.19	0.357	53.21	0.847	83.61
	E2E+Sampling	0.848	50.73	0.357	50.14	0.864	82.78
	TPSR ($\lambda=0$)	0.952	84.42	0.928	82.78	0.938	129.85
	TPSR ($\lambda=0.1$)	0.949	57.22	0.785	56.14	0.945	95.71
	TPSR ($\lambda=0.5$)	0.924	50.01	0.714	47.02	0.931	82.58
	TPSR ($\lambda=1$)	0.916	47.24	0.571	43.42	0.924	79.43

Data Group	Model	$\uparrow R^2 > 0.99$	$\uparrow R^2$	$\uparrow Acc_{0.1}$	$\uparrow Acc_{0.01}$	$\uparrow Acc_{0.001}$	$\downarrow Complexity$
In-domain	E2E+Beam	0.657	0.782	0.461	0.298	0.2	38.37
	E2E+Sampling	0.640	0.794	0.472	0.332	0.208	39.82
	TPSR ($\lambda=0$)	0.702	0.828	0.550	0.416	0.333	67.11
	TPSR ($\lambda=0.1$)	0.708	0.833	0.514	0.326	0.213	40.31
	TPSR ($\lambda=0.5$)	0.697	0.830	0.459	0.274	0.184	36.55
	TPSR ($\lambda=1$)	0.691	0.827	0.439	0.271	0.176	35.67

Table 1: Performance of TPSR compared with beam search and sampling decoding strategies on the SRBench [25], and In-domain Synthetic [18] datasets.

more than 200 points, we follow [18] and use B bags of data, each containing $N = 200$ points, due to the limitation that the baseline method is pretrained with $N \leq 200$ data points. In the baseline method [18], a total of BC candidates are generated (C candidates for B bags), which are then sorted and refined to generate the best equation. However, for TPSR, since we need to train an MCTS for each bag, we use an iterative decoding approach, starting with the first bag and continuing with subsequent bags until a criterion ($R^2 > 0.99$) is met or we use a maximum of $B = 10$ bags. To ensure a fair comparison, we use $B = 10$ for the E2E baseline method as well. In this table, we demonstrate the results of our proposed framework, TPSR, with varying values of the λ parameter that controls the trade-off between fitting performance and complexity in the hybrid reward function defined in Eq. (1). As shown in Table 1 and Fig. 5(a), when $\lambda = 0$, the framework generates complex equations that overoptimize for fitting performance. However, as we increase λ , the framework generates less complex equations with a slight reduction in fitting performance. Notably, even for large values of λ , such as $\lambda = 1$, the fitting performance of TPSR significantly outperforms that of the baseline methods. Therefore, these findings demonstrate that TPSR outperforms the baseline methods over different datasets in terms of fitting performance across all datasets, while also generating equations that are comparable or less complex than those generated by the baseline methods. Table 1 shows that TPSR exhibits a more significant gap in fitting performance when compared to E2E on SRBench datasets, while this gap is smaller for In-domain datasets (even performing slightly worse on Acc_w for larger $\lambda = 0.5, 1$). This is due to the In-domain dataset being generated using the same approach as the E2E pretraining data, resulting in the E2E model’s superior performance on this dataset.

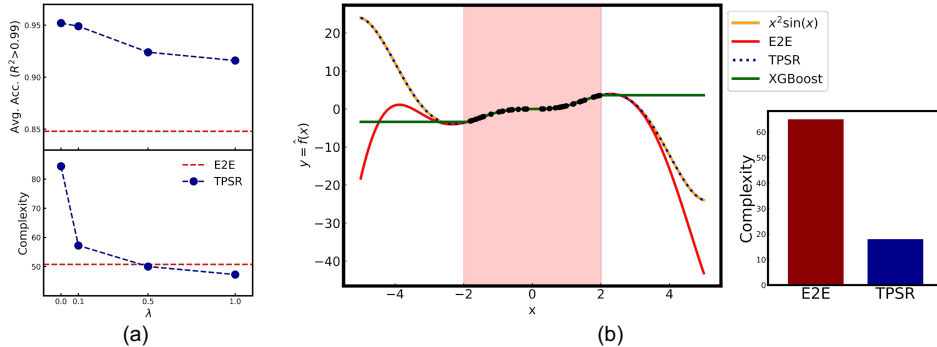


Figure 5: (a) Effect of controllable complexity parameter (λ) on average test performance and equation complexity for the *Feynman* dataset. (b) Qualitative comparison of TPSR with E2E as well as black-box XGBoost [45] fitting. The training dataset contains 200 points in range of $(-2, 2)$ (shaded region), and the performance is evaluated over $(-5, 5)$. E2E uses sampling decoding in both subfigures.

Figure 5(b) provides a qualitative comparison between the performance of TPSR, the E2E baseline (symbolic model), and XGBoost [45] (black-box model), with regards to the ground-truth equation

$x^2 \sin(x)$. The training dataset, represented by the shaded region, comprises 200 data points in the range of $(-2, 2)$, and the evaluation is conducted on the out-of-domain region between $(-5, 5)$. Although all three models fit the training data very well, our proposed TPSR approach outperforms the E2E baseline in fitting the underlying true function, as shown by the out-of-domain performance. This may be attributed to TPSR’s ability to generate less complex equations that effectively fit the data, as illustrated in the complexity barplot. Additionally, the results indicate that symbolic regression methods generally provide a better fit to the underlying function compared to black-box XGBoost ML method over the unseen evaluation range.

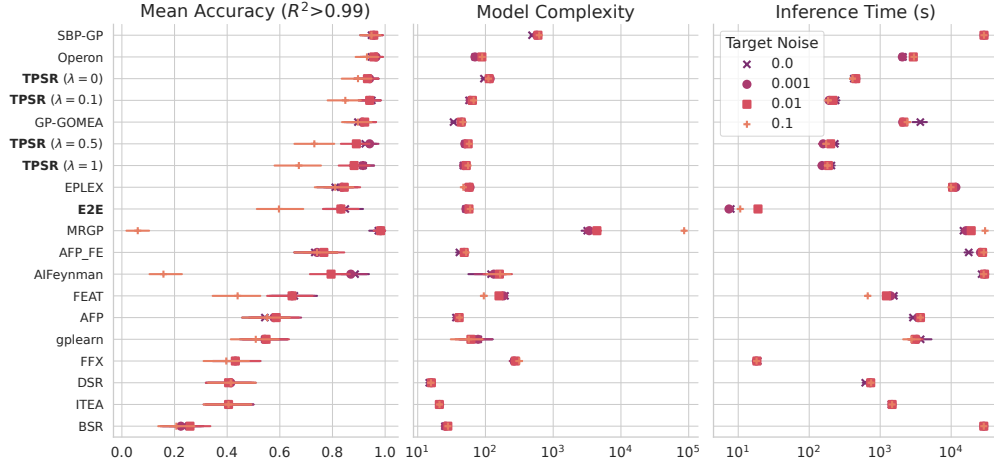


Figure 6: Performance comparison of TPSR and SRBench algorithms in terms of Accuracy-Complexity-Time on *Feynman* dataset. Algorithms are sorted based on mean accuracy defined as the ratio of solutions with $R^2 > 0.99$ on test set under various noise levels. TPSR demonstrates a strong balance of performance with relatively low model complexity and lower inference time compared to GP-based algorithms. The error bars represent the 95% confidence interval.

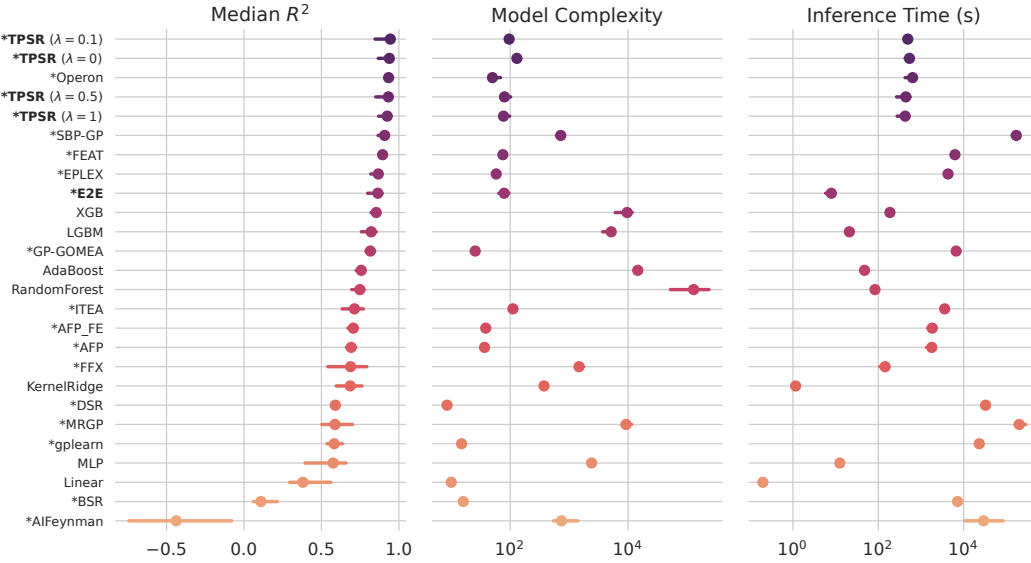


Figure 7: Performance comparison of TPSR and SRBench algorithms in terms of Accuracy-Complexity-Time on *Black-box* dataset. Algorithms are sorted based on median R^2 score on test set. TPSR ($\lambda = 0, 0.1$) achieves the best fitting performance while having a controllable complexity and lower inference time compared to the GP-based SR algorithms. The error bars represent the 95% confidence interval and "*" refers to SR methods.

Figures 6 and 7 present a detailed comparison of our proposed TPSR with the baseline E2E transformer model and all the SRBench baselines on the PMLB *Feynman* and *Black-box* datasets, respectively. These figures illustrate the relative position of each algorithm with respect to (1) fitting

performance, (2) model complexity, and (3) inference time. The results indicate that transformer-based planning in the TPSR significantly enhances the performance of E2E and outperforms even the state-of-the-art baselines, achieving the highest fitting performance on the black-box datasets. This is achieved while the complexity of the generated equations in TPSR is not greater than that of E2E, and shows a great fitting-complexity balance compared to other SR algorithms. The pareto plots provided in Fig. 1 also demonstrate the effectiveness of our TPSR in balancing fitting and complexity compared to all other SRBench baselines. Our TPSR effectively pushes this balanced performance to the first pareto front for both the *Feynman* and *Black-box* datasets. Moreover, it is important to note that, while the inference time of our TPSR is longer than the baseline E2E transformer model, it still has comparable or lower inference time than most of the SRBench baselines.

4.2.2 (RQ2) Extrapolation and Noise Robustness

The ability to extrapolate well is inherently linked to the quality of the equation obtained through symbolic regression. To investigate the extrapolation performance of TPSR to out-of-training regions, we normalize the input test data points to different scales (σ) instead of unit variance (used for training points) as per [18]. Figure 8(a) depicts the average performance of TPSR compared to E2E with the sampling decoding on the training data as well as testing data in scales of $\sigma = \{1, 2, 4, 8, 16\}$ for the *In-domain Synthetic* datasets. Also, we investigate the effect of different complexity controlling levels ($\lambda = \{0, 0.1, 0.5, 1.0\}$) on the extrapolation performance. It can be observed that, while $\lambda = 0$ (i.e., no complexity regularization) achieves the best fitting accuracy on the training data, it has a sub-par performance for $\sigma > 8$. This can be due to the overfitting issue when the symbolic model is much more complex than the real complexity of the equation, similar to the common overfitting issue in ML models. The results highlight the importance of controlling complexity in the extrapolation of identified equations. For values of $\lambda > 0$, the overfitting issue is mitigated as the generated equations become less complex. However, very high values of λ (e.g., $\lambda = 1$) can result in poor fitting performance. The flexibility of TPSR for allowing different values of λ to balance fitting and complexity for a given task is crucial for optimal performance.

Figure 8(b) also presents the robustness of TPSR with different λ levels compared to the E2E transformer baseline on the *Feynman* dataset. The results indicate that MCTS-guided decoding can offer robust performance with a smaller drop compared to the baseline in the presence of noise.

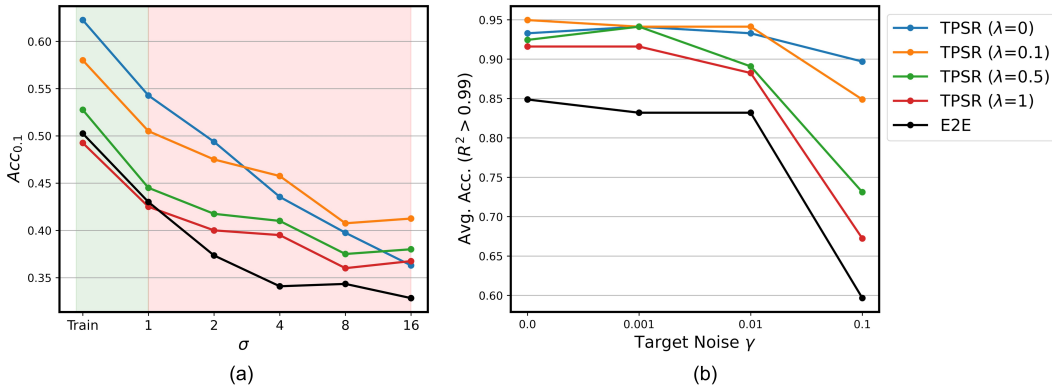


Figure 8: TPSR with λ range in $\{0, 0.1, 0.5, 1\}$ compared to E2E using sampling for (a) **Extrapolation performance** where in-domain accuracy is shown for different input variances (σ), and (b) **Robustness to noise**, where mean accuracy ($R^2 > 0.99$) is shown for various target noise levels (γ).

4.2.3 Ablation Study

To investigate the effect of different parameters and modules on the performance of TPSR, we perform ablative experiments with different variants of our model, including different MCTS parameters such as *rollout*, *k_{max}*, and *b*, as well as different caching mechanisms. All ablation experiments are performed on the *Feynman* datasets and results are reported in Fig. 9.

(RQ3) Caching Mechanisms. In Figure 9(a), we illustrate the effectiveness of the sequence and *top-k* caching mechanisms in reducing the total inference time of our TPSR framework for MCTS-guided decoding. Our experiments show that sequence caching has more effect in dropping the

inference time as it replaces the time-consuming sequence generation process for the entire equation sequence. Additionally, *top-k* caching can also slightly reduce the inference time by storing and suggesting the next most likely tokens, eliminating the need to call the transformer repeatedly to obtain these values in each MCTS iteration. Overall, these two mechanisms can reduce the total inference time by around 28%.

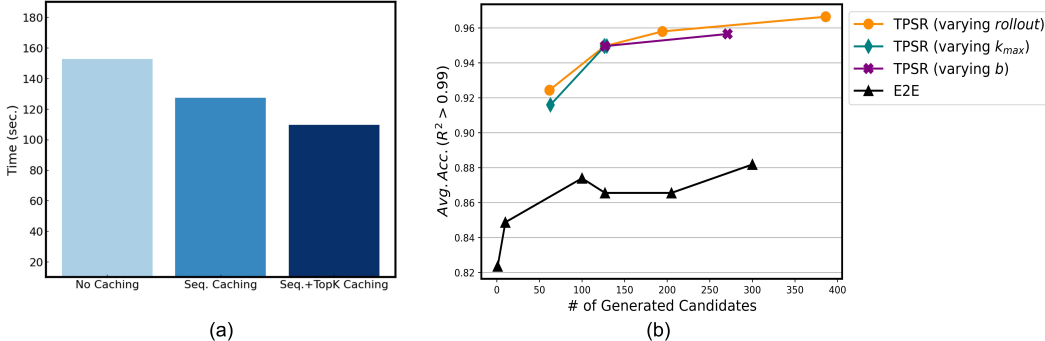


Figure 9: Ablation study on the modules and parameters of TPSR. **(a) Effect of caching mechanisms:** Sequence caching and *top-k* caching improve the inference time of TPSR ($\lambda = 0.1$). **(b) Efficiency and parameters of TPSR:** Average accuracy of TPSR (varying model parameters), and baseline E2E (varying sampling size) vs. number of generated candidates.

(RQ4) Search Parameters. Fig. 9(b) shows the fitting performance vs. the number of generated equations throughout the decoding process for both TPSR ($\lambda = 0.1$) and the baseline E2E with sampling decoding. For this study, we evaluated the number of generation samples in E2E with values of $C = K = 1, 10, 100, 127, 205, 300$ based on the average number of generated samples for various settings of TPSR. The results show that under the same number of generated equation candidates, TPSR significantly outperforms the E2E baseline. This is primarily attributed to the fact that the E2E baseline is deprived of any feedback on the fitting performance of the generated equations, and solely relies on the token-generation probabilities obtained through pretraining. We report the results for variants of our TPSR with different MCTS parameters. We assess the performance with varying number of rollouts, $r = \{3, 6, 9\}$, number of beams in simulations, $b = \{1, 3\}$, and the maximum number of possible expansions at each state, $k_{max} = \{2, 3, 4\}$. The default setting of TPSR parameters are $b = 1$, $k_{max} = 3$, and $r = 3$. The results indicate that increasing r , k_{max} , and b all contribute to the better performance of TPSR, with the most significant improvement observed when increasing r . This is because more rollouts provide the model with more opportunities to learn from trials and learn better values.

5 Conclusion

In this work, we propose TPSR, a model-agnostic decoding strategy for symbolic regression that leverages the power of pretrained SR transformer models and MCTS algorithm to explore the space of possible equations based on the objective designed for equation fitting and complexity. Our experimental results demonstrate the superiority of TPSR over existing methods in terms of generating equations with a better fitting-complexity trade-off on multiple benchmark datasets. We show that TPSR is flexible in controlling the equation complexity level for a given task without the need for finetuning and updating the pretrained model. Our work is the first to incorporate performance feedback as an external source of knowledge in the generation process of pretrained SR models. We hope that this work can inspire further research into the integration of pretrained models with planning or reinforcement learning algorithms. In the future, we would like to explore alternative ways of updating the baseline transformer model weights, relax equation generation by pretrained models, and improve search efficiency through methods like parallel MCTS.

References

- [1] He Ma, Arunachalam Narayanaswamy, Patrick Riley, and Li Li. Evolving symbolic density functionals. *Science Advances*, 8(36):eabq0279, 2022.
- [2] Yiqun Wang, Nicholas Wagner, and James M. Rondinelli. Symbolic regression in materials science. *MRS Communications*, 9(3):793–805, 2019.
- [3] Samuel H. Rudy, Steven L. Brunton, Joshua L. Proctor, and J. Nathan Kutz. Data-driven discovery of partial differential equations. *Science Advances*, 3(4):e1602614, 2017.
- [4] Kazem Meidani and Amir Barati Farimani. Data-driven identification of 2d partial differential equations using extracted physical features. *Computer Methods in Applied Mechanics and Engineering*, 381:113831, 2021.
- [5] Steven L. Brunton, Joshua L. Proctor, and J. Nathan Kutz. Discovering governing equations from data by sparse identification of nonlinear dynamical systems. *Proceedings of the National Academy of Sciences*, 113(15):3932–3937, 2016.
- [6] Miles Cranmer, Alvaro Sanchez-Gonzalez, Peter Battaglia, Rui Xu, Kyle Cranmer, David Spergel, and Shirley Ho. Discovering symbolic models from deep learning with inductive biases. In *Proceedings of the 34th International Conference on Neural Information Processing Systems*, NIPS’20, Red Hook, NY, USA, 2020.
- [7] E. Kaiser, J. N. Kutz, and S. L. Brunton. Sparse identification of nonlinear dynamics for model predictive control in the low-data limit. *Proceedings of the Royal Society A: Mathematical, Physical and Engineering Sciences*, 474(2219):20180335, 2018.
- [8] Kazem Meidani and Amir Barati Farimani. Identification of parametric dynamical systems using integer programming. *Expert Systems with Applications*, 219:119622, 2023.
- [9] Yoshitomo Matsubara, Naoya Chiba, Ryo Igarashi, Taniai Tatsunori, and Yoshitaka Ushiku. Rethinking symbolic regression datasets and benchmarks for scientific discovery. *arXiv preprint arXiv:2206.10540*, 2022.
- [10] Marco Virgolini and Solon P Pissis. Symbolic regression is NP-hard. *Transactions on Machine Learning Research*, 2022.
- [11] Haoran Li, Yang Weng, and Hanghang Tong. CoNSole: Convex neural symbolic learning. In Alice H. Oh, Alekh Agarwal, Danielle Belgrave, and Kyunghyun Cho, editors, *Advances in Neural Information Processing Systems*, 2022.
- [12] Michael Schmidt and Hod Lipson. Distilling free-form natural laws from experimental data. *Science Advance*, 324(5923):81–85, 2009.
- [13] Bogdan Burlacu, Gabriel Kronberger, and Michael Kommenda. Operon c++: An efficient genetic programming framework for symbolic regression. In *Proceedings of the 2020 Genetic and Evolutionary Computation Conference Companion*, GECCO ’20, page 1562–1570, New York, NY, USA, 2020. Association for Computing Machinery.
- [14] Brenden K Petersen, Mikel Landajuela Larra, Terrell N. Mundhenk, Claudio Prata Santiago, Soo Kyung Kim, and Joanne Taery Kim. Deep symbolic regression: Recovering mathematical expressions from data via risk-seeking policy gradients. In *International Conference on Learning Representations*, 2021.
- [15] Ashish Vaswani, Noam Shazeer, Niki Parmar, Jakob Uszkoreit, Llion Jones, Aidan N Gomez, Łukasz Kaiser, and Illia Polosukhin. Attention is all you need. In *Advances in Neural Information Processing Systems*, volume 30, 2017.
- [16] Luca Biggio, Tommaso Bendinelli, Alexander Neitz, Aurelien Lucchi, and Giambattista Parascandolo. Neural symbolic regression that scales. In Marina Meila and Tong Zhang, editors, *Proceedings of the 38th International Conference on Machine Learning*, volume 139 of *Proceedings of Machine Learning Research*, pages 936–945. PMLR, 18–24 Jul 2021.
- [17] Mojtaba Valipour, Bowen You, Maysum Panju, and Ali Ghodsi. Symbolicgpt: A generative transformer model for symbolic regression. *arXiv preprint arXiv:2106.14131*, 2021.
- [18] Pierre-Alexandre Kamienny, Stéphane d’Ascoli, Guillaume Lample, and Francois Charton. End-to-end symbolic regression with transformers. In *Advances in Neural Information Processing Systems*, 2022.

- [19] Martin Vastl, Jonáš Kulhánek, Jirí Kubalík, Erik Derner, and Robert Babuška. Symformer: End-to-end symbolic regression using transformer-based architecture. *arXiv preprint arXiv:2205.15764*, 2022.
- [20] Roger Fletcher. *Practical Methods of Optimization*. John Wiley & Sons, New York, NY, USA, second edition, 1987.
- [21] Alex Graves. Sequence transduction with recurrent neural networks. *arXiv preprint arXiv:1211.3711*, 2012.
- [22] Sam Wiseman and Alexander M. Rush. Sequence-to-sequence learning as beam-search optimization. In *Proceedings of the 2016 Conference on Empirical Methods in Natural Language Processing*, pages 1296–1306, Austin, Texas, November 2016. Association for Computational Linguistics.
- [23] Angela Fan, Mike Lewis, and Yann Dauphin. Hierarchical neural story generation. In *Proceedings of the 56th Annual Meeting of the Association for Computational Linguistics (Volume 1: Long Papers)*, pages 889–898, Melbourne, Australia, jul 2018. Association for Computational Linguistics.
- [24] Silviu-Marian Udrescu and Max Tegmark. Ai feynman: A physics-inspired method for symbolic regression. *Science Advances*, 6(16):eaay2631, 2020.
- [25] William La Cava, Patryk Orzechowski, Bogdan Burlacu, Fabricio de Franca, Marco Virgolin, Ying Jin, Michael Kommenda, and Jason Moore. Contemporary symbolic regression methods and their relative performance. In J. Vanschoren and S. Yeung, editors, *Proceedings of the Neural Information Processing Systems Track on Datasets and Benchmarks*, volume 1, 2021.
- [26] Allan Costa, Rumen Dangovski, Owen Dugan, Samuel Kim, Pawan Goyal, Marin Soljačić, and Joseph Jacobson. Fast neural models for symbolic regression at scale. *arXiv preprint arXiv:2007.10784*, 2020.
- [27] Mikel Landajuela, Brenden K Petersen, Sookyung Kim, Claudio P Santiago, Ruben Glatt, Nathan Mundhenk, Jacob F Pettit, and Daniel Faissol. Discovering symbolic policies with deep reinforcement learning. In Marina Meila and Tong Zhang, editors, *Proceedings of the 38th International Conference on Machine Learning*, volume 139, pages 5979–5989. PMLR, 18–24 Jul 2021.
- [28] Terrell N. Mundhenk, Mikel Landajuela, Ruben Glatt, Claudio P. Santiago, Daniel faissol, and Brenden K. Petersen. Symbolic regression via deep reinforcement learning enhanced genetic programming seeding. In A. Beygelzimer, Y. Dauphin, P. Liang, and J. Wortman Vaughan, editors, *Advances in Neural Information Processing Systems*, 2021.
- [29] Fangzheng Sun, Yang Liu, Jian-Xun Wang, and Hao Sun. Symbolic physics learner: Discovering governing equations via monte carlo tree search. In *The Eleventh International Conference on Learning Representations*, 2023.
- [30] Jacob Devlin, Ming-Wei Chang, Kenton Lee, and Kristina Toutanova. BERT: Pre-training of deep bidirectional transformers for language understanding. In *Proceedings of the 2019 Conference of the North American Chapter of the Association for Computational Linguistics: Human Language Technologies, Volume 1 (Long and Short Papers)*, pages 4171–4186, Minneapolis, Minnesota, June 2019. Association for Computational Linguistics.
- [31] Tom Brown, Benjamin Mann, Nick Ryder, Melanie Subbiah, Jared D Kaplan, Prafulla Dhariwal, Arvind Neelakantan, Pranav Shyam, Girish Sastry, Amanda Askell, Sandhini Agarwal, Ariel Herbert-Voss, Gretchen Krueger, Tom Henighan, Rewon Child, Aditya Ramesh, Daniel Ziegler, Jeffrey Wu, Clemens Winter, Chris Hesse, Mark Chen, Eric Sigler, Mateusz Litwin, Scott Gray, Benjamin Chess, Jack Clark, Christopher Berner, Sam McCandlish, Alec Radford, Ilya Sutskever, and Dario Amodei. Language models are few-shot learners. In H. Larochelle, M. Ranzato, R. Hadsell, M.F. Balcan, and H. Lin, editors, *Advances in Neural Information Processing Systems*, volume 33, pages 1877–1901. Curran Associates, Inc., 2020.
- [32] Yue Wang, Weishi Wang, Shafiq Joty, and Steven C.H. Hoi. CodeT5: Identifier-aware unified pre-trained encoder-decoder models for code understanding and generation. In *Proceedings of the 2021 Conference on Empirical Methods in Natural Language Processing*, pages 8696–8708, Online and Punta Cana, Dominican Republic, November 2021. Association for Computational Linguistics.

- [33] Thomas Scialom, Paul-Alexis Dray, Jacopo Staiano, sylvain lamprier, and Benjamin Piwowarski. To beam or not to beam: That is a question of cooperation for language GANs. In A. Beygelzimer, Y. Dauphin, P. Liang, and J. Wortman Vaughan, editors, *Advances in Neural Information Processing Systems*, 2021.
- [34] Rémi Leblond, Jean-Baptiste Alayrac, Laurent Sifre, Miruna Pislari, Lespiau Jean-Baptiste, Ioannis Antonoglou, Karen Simonyan, and Oriol Vinyals. Machine translation decoding beyond beam search. In *Proceedings of the 2021 Conference on Empirical Methods in Natural Language Processing*, pages 8410–8434, Online and Punta Cana, Dominican Republic, November 2021. Association for Computational Linguistics.
- [35] Antoine Chaffin, Vincent Claveau, and Ewa Kijak. PPL-MCTS: Constrained textual generation through discriminator-guided MCTS decoding. In *Proceedings of the 2022 Conference of the North American Chapter of the Association for Computational Linguistics: Human Language Technologies*, pages 2953–2967, Seattle, United States, July 2022. Association for Computational Linguistics.
- [36] Xinyun Chen, Chang Liu, and Dawn Song. Execution-guided neural program synthesis. In *International Conference on Learning Representations*, 2019.
- [37] Parshin Shojaee, Kazem Meidani, Amir Barati Farimani, and Chandan K Reddy. Transformer-based planning for symbolic regression. *arXiv preprint arXiv:2303.06833*, 2023.
- [38] Shun Zhang, Zhenfang Chen, Yikang Shen, Mingyu Ding, Joshua B. Tenenbaum, and Chuang Gan. Planning with large language models for code generation. In *International Conference on Learning Representations*, 2023.
- [39] Guillaume Lample and François Charton. Deep learning for symbolic mathematics. In *International Conference on Learning Representations*, 2020.
- [40] Levente Kocsis and Csaba Szepesvári. Bandit based monte-carlo planning. In Johannes Fürnkranz, Tobias Scheffer, and Myra Spiliopoulou, editors, *Machine Learning: ECML 2006*, pages 282–293, Berlin, Heidelberg, 2006. Springer Berlin Heidelberg.
- [41] Silviu-Marian Udrescu, Andrew Tan, Jiahai Feng, Orisvaldo Neto, Tailin Wu, and Max Tegmark. Ai feynman 2.0: Pareto-optimal symbolic regression exploiting graph modularity. In H. Larochelle, M. Ranzato, R. Hadsell, M.F. Balcan, and H. Lin, editors, *Advances in Neural Information Processing Systems*, volume 33, pages 4860–4871. Curran Associates, Inc., 2020.
- [42] Randal S. Olson, William La Cava, Patryk Orzechowski, Ryan J. Urbanowicz, and Jason H. Moore. Pmlb: a large benchmark suite for machine learning evaluation and comparison. *BioData Mining*, 10(1):36, Dec 2017.
- [43] William La Cava, Kourosh Danai, and Lee Spector. Inference of compact nonlinear dynamic models by epigenetic local search. *Engineering Applications of Artificial Intelligence*, 55:292–306, 2016.
- [44] Stéphane D’Ascoli, Pierre-Alexandre Kamienny, Guillaume Lample, and Francois Charton. Deep symbolic regression for recurrence prediction. In Kamalika Chaudhuri, Stefanie Jegelka, Le Song, Csaba Szepesvari, Gang Niu, and Sivan Sabato, editors, *Proceedings of the 39th International Conference on Machine Learning*, volume 162 of *Proceedings of Machine Learning Research*, pages 4520–4536. PMLR, 17–23 Jul 2022.
- [45] Tianqi Chen and Carlos Guestrin. XGBoost: A scalable tree boosting system. In *Proceedings of the 22nd ACM SIGKDD International Conference on Knowledge Discovery and Data Mining*, KDD ’16, pages 785–794, New York, NY, USA, 2016. ACM.